ORIGINAL ARTICLE

INTERNATIONAL JOURNAL OF RESEARCH IN PHARMACEUTICAL SCIENCES

Published by JK Welfare & Pharmascope Foundation Journal Home Page: www.ijrps.com

Synthesis and Characterization of CSNP-SiO_2 nanocomposite by using antibacterial activity

Rajaduraipandian Subramanian[1], Amutha Eswaran[2], Gandhimathi Sivasubramanian[1], Annadurai Gurusamy*[2]

[1]Sri Paramakalyani College, Manonmaniam Sundaranar University, Alwarkurichi - 627412, Tamil Nadu, India

[2]Sri Paramakalyani Centre of Excellence in Environmental Sciences, Manonmaniam Sundaranar University, Alwarkurichi – 627412, Tamil Nadu, India

Article History:

Received on: 26 Sep 2021
Revised on: 18 Nov 2021
Accepted on: 28 Dec 2021

Keywords:

Chitosan,
chitosan NPs,
CSNP - SiO2 nanocomposite,
Antibacterial activity,
TGA,
XRD,
SEM

ABSTRACT

Because of its promising biological achievements, the development of nanotechnology, nanoparticle-based products, and their applications has piqued the interest of many researchers. Inorganic nanomaterials, on the other hand, are well known to be effective antimicrobial agents. Metal nanoparticles, such as Silicon dioxide, are particularly important among the various nanoparticles due to their low cost and ease of availability. Chitosan is a biopolymer derived from chitin, a natural polysaccharide that follows cellulose as the second most abundant polysaccharide. The Precipitation Method was used to create a Chitosan Nanoparticle with SiO_2 Nanocomposite (CSNP - SiO_2 nanocomposite). TGA, XRD, SEM, FT-IR, PSA, UV, and FL were used to characterize the Chitosan Nanoparticle with SiO_2 Nanocomposite. The findings showed that bionanocomposites have a greater antibacterial effect due to the combined effect of CS and nanoparticles (NPs). Chitosan/SiO_2 nanocomposites were tested for antimicrobial activity against gram-positive and gram-negative microorganisms. The goal was to assess their physical, mechanical, and biological properties, as well as their potential for biomedical applications.

*Corresponding Author

Name: Annadurai Gurusamy
Phone: 9442027196
Email: annananoteam@gmail.com

ISSN: 0975-7538

DOI: https://doi.org/10.26452/ijrps.v13i2.187

Production and Hosted by

IJRPS | www.ijrps.com

INTRODUCTION

Nanobiotechnology has emerged as a fundamental field of current research as a cutting-edge innovation that is interdisciplinary with physics, chemistry, and biology [1, 2]. During the last decade, nanomaterials demonstrated significant antimicrobial activity against human, animal, and plant pathogens [3]. Researchers refer to this potential as their distinct optical, electronic, or mechanical properties because of quantum and surface boundary effects compared to bulk materials [4]. Nanocomposite materials have been used in various applications, including wound healing, tissue engineering, thermal therapy, and drug delivery [5]. Chitosan is a biocompatible polymer made up of polysaccharide with antibacterial properties that has been used in wound dressings [6]. Chitosan is a biopolymer composed of N-acetylglucosamine and glucosamine. It has many properties, including non-toxicity, biocompatibility, biodegradability, moisture retention, and low cost [7–9]. The antimicrobial activity of chitosan polymers and nanoparticles can be attributed primarily to their electric charge and high adsorption ability, as well as chem-

ical reactions that allow them to interact efficiently with the bacterial cell membrane [10, 11], whereas the inhibitory effect on bacterial growth is dependent on their sizes and shapes, as well as biological properties [10, 12]. When chitosan and metal nanoparticles are combined, their antibacterial activity may be significantly inhibited compared to the antibacterial activity of chitosan and metal nanoparticles alone (Diagram 1). Chitosan has been studied as the primary structural unit of nanomaterials due to its low toxicity, non-immunogenicity, and biodegradability. Li et al. (2010) [13], for example, A chitosan/TiO_2 nanocomposite with antibacterial activity against *Xanthomonas oryzae PV. oryzae* was synthesised and characterised. In this study, we report on the preparation of a silicon dioxide – chitosan nanocomposite by chemical reduction of corresponding metal ions into zero valent nanoparticles in the presence of chitosan. The morphology of these nanocomposites was studied in addition to their optical and other properties. Antibacterial activity was evaluated against five gram-positive (*Bacillus subtilis and Staphylococcus aureus*) and gram-negative microorganisms (*Enterobacter, Escherichia coli and Pseudomonas fluorescens*).

MATERIALS AND METHODS

CDH Chemicals New Delhi supplied the following analytical grade chemicals: silicon dioxide (SiO_2), Chitosan, sodium tripolyphosphate (STPP), sodium hydroxide, potassium permanganate, oxalic acid, acetic acid, hydrochloric acid, and sodium hydroxide.

Synthesis of Chitosan nanoparticle

The method of ionic gelation was used to create chitosan nanoparticles from chitosan. To make a chitosan solution, 0.5g of chitosan was dissolved in 5% acetic acid and stirred for 30 minutes. Sodium tripolyphosphate, a cross-linking agent, was added dropwise. A magnetic stirrer was used to mix the mixture at the same time. After stirring at room temperature, the solution was centrifuged for 30 minutes and kept in a hot air oven to obtain chitosan nanoparticle powder. Chitosan nanoparticles were created from the white powder that was obtained.

Synthesis of CSNP-SiO_2 nanocomposite

0.5g of Chitosan nanoparticles were mixed with 100 ml of distilled water, and the solution was supplemented with 0.5g of SiO_2, as shown in Figure 1. To keep the reaction going, constant stirring was used. The reaction was kept going for about 2-4 hours. After that, it was centrifuged for 30 minutes and dried in a hot air oven at 1000 degrees Fahrenheit. The powder was ground with a mortar and pestle and calcined for 8000 seconds to produce a CSNP-SiO_2 nanocomposite.

Antibacterial Property

The agar diffusion method was used to test the antibacterial activity of CSNP-SiO_2 nanocomposite against the bacterial strains *Staphylococcus aureus, Bacillus subtilus, Enterobacter, Escherichia coli and Pseudomonas fluorescens.* Bacterial strains were grown overnight on a rotary shaker in a Nutrient broth medium in a single column system. The same is kept for 24 hours in a sophisticated incubator for incubation. To determine the bacterial effect of the CSNP-SiO_2 nanocomposite, a loop of bacterial culture was placed on the Muller Hinton broth medium. After 24 hours, the zones of inhibition were measured under the same conditions.

RESULTS AND DISCUSSION

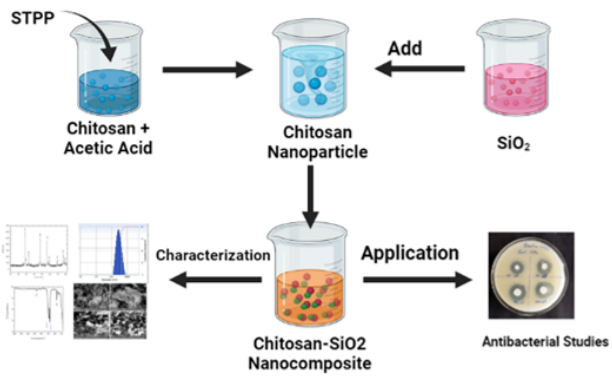

Diagram 1: Graphical Abstract

Figure 1: Synthesis of CSNP-SiO_2 nanocomposite

XRD Diffraction

The CSNP-SiO_2 XRD pattern (Figure 2) revealed ultrafine powder samples obtained from sol. The result shows an amorphous structure rather than a crystalline structure. The crystalline structure was expected to result from the sample being heat treated at a high calcination temperature (i.e.,50°c).

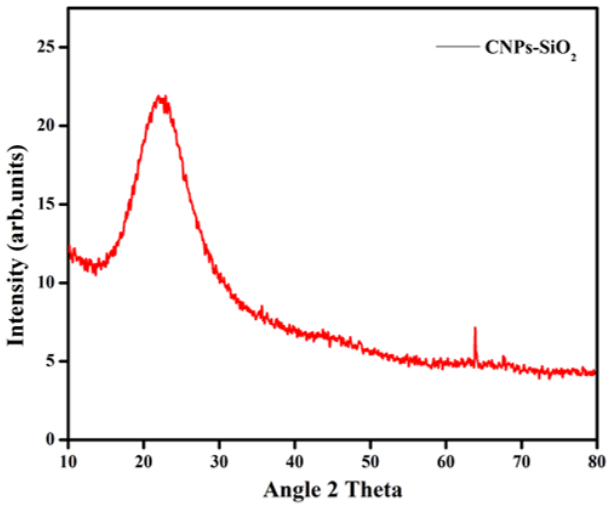

Figure 2: X-ray diffraction (XRD) analysis of CSNP-SiO_2

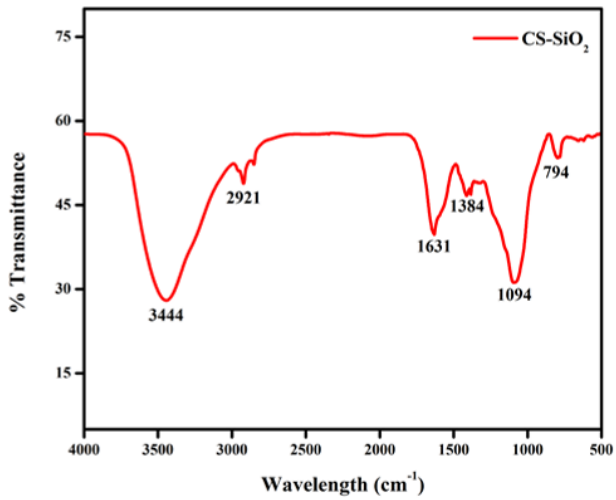

Figure 3: FTIR spectra of CSNP-SiO_2 nanocomposite

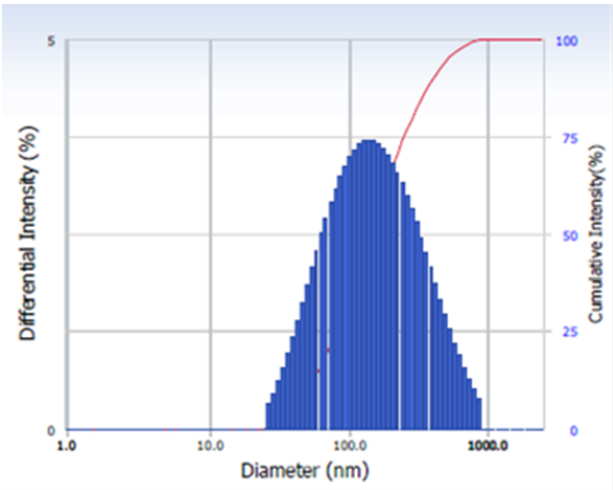

Figure 4: The particle size and distribution of CSNP-SiO_2

The diffractogram (Figure 2) was compared to the JCPDS standard powder diffraction card, CSNP-SiO_2 file No. 00-001-1262. CSNPs are amorphous with no crystalline peak in the XRD pattern, but when incorporated with SiO_2, they exhibited characteristic crystalline peaks at 2 values of 22.91° and 64.95°, corresponding to (hkl) values - (111) and (200) planes of CSNP-SiO_2. The XRD analysis confirmed that the particles in the prepared sample are CSNP-SiO_2 with a face-centred cubic crystal structure [14]. As the peak intensity of polymer nanocomposite films increases, the amorphous nature of polymer nanocomposite films decreases, while the semi-crystalline nature of polymer nanocomposite films increases [15]. The stable structure of the hydrogen bonds between water molecules and the amino groups of chitosan has previously been reported, as the water, molecules are due to the crystalline region of chitosan [15].

Fourier-transform infrared spectroscopy

The bonding nature of the CSNP-SiO_2 nanocomposite was investigated using an infrared analysis tool. Figure 3 depicts the FT-IR spectra of a CSNP-SiO_2 nanocomposite. The samples' IR spectrum was examined at wavelengths ranging from 4000 to 400 cm^{-1}. The peak at 3444 cm^{-1} was more prominent than the others, indicating -NH2 and -OH stretching primary amines. The presence of C–H stretch alkanes was suggested by the peak 2921 cm^{-1} [10]. Peak 1631 cm^{-1} indicates the presence of C=C stretching alkene, while 1094 cm^{-1} indicates C-O stretching aliphatic ether and 794 cm^{-1} indicates the presence of C=C bending alkene compound. Previous studies Wang et al. (2020) reported similar results for the formation of chitosan nanoparticles treated TPP. The FTIR spectral absorbance of CSNP-SiO_2 nanocomposite shows all of the SiO_2 and biopolymer chitosan vibrations. The observed functional groups indicated that chitosan might be responsible for the reduction and formation of SiO_2, and the other chitosan functional groups present in CSNP-SiO_2 nanocomposite support chitosan coating on synthesized CSNP-SiO_2 nanocomposite. The FTIR spectral absorbance of the CSNP-SiO_2 nanocomposite shows that all the SiO_2 and biopolymer chitosan vibrations are present. The observed functional groups suggested that chitosan may be responsible for SiO_2 reduction and formation, and the other chitosan functional groups present in CSNP-SiO_2 nanocomposite support chitosan coating on synthesised CSNP-SiO_2 nanocomposite [16]. FT-IR techniques are one of the most effective methods for investigating interactions between a polymer matrix and a CSNP-SiO_2 nanocomposite material.

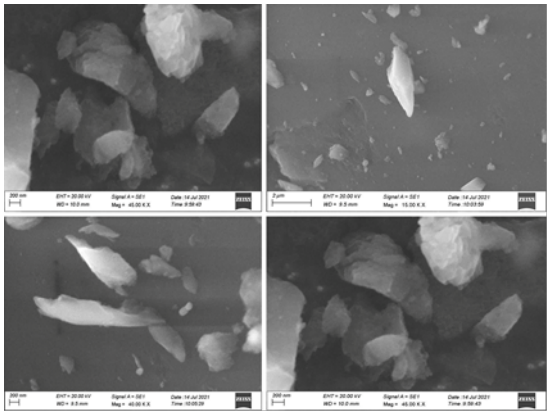

Figure 5: Represents the SEM image of CSNP-SiO_2

The mechanical properties of the CSNP-SiO_2 nanocomposite can be explained using a detailed analysis of FT-IR spectra.

The formation of hydrogen bonds and van der Waals interactions between the phases increased the mechanical parameters of the nanocomposite material [17].

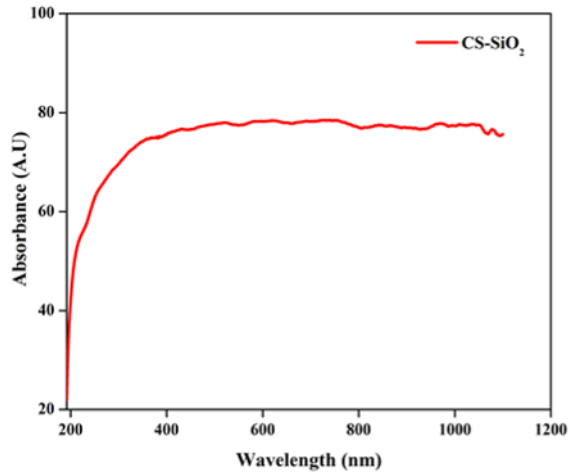

Figure 6: Absorption spectra of CSNP-SiO_2

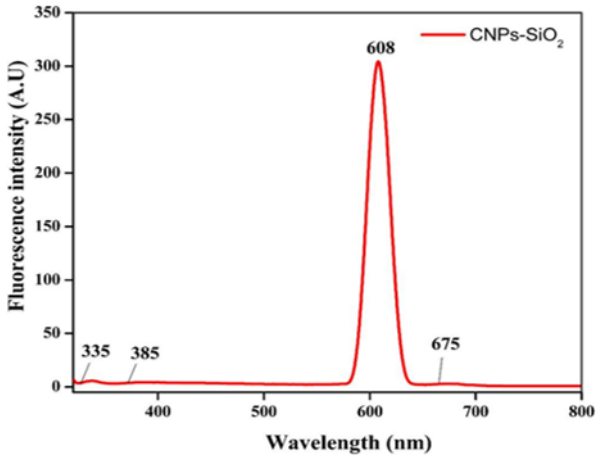

Figure 7: Fluorescence spectra of CSNP-SiO_2

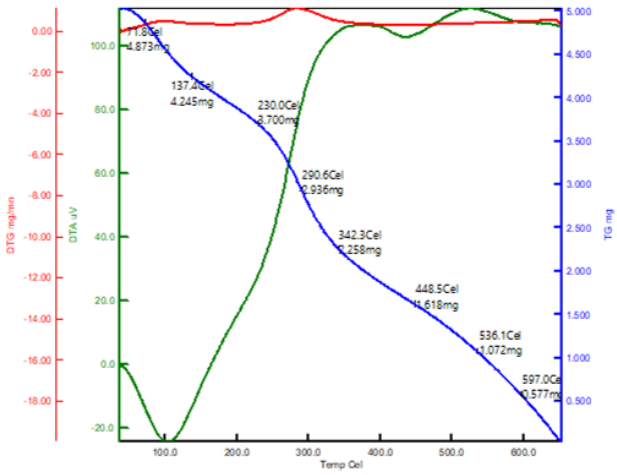

Figure 8: TGA curve of CSNP-SiO_2

Particle Size Analyzer

The diameter of nanoparticles dispersed in liquid is measured using the DLS, as shown in Figure 4. It also determines particle size and distribution in physiological solutions. DLS can measure the size distribution of small particles in solution or suspension on a scale ranging from submicron to one nanometer [18]. This method can measure narrow particle size distributions, particularly in the 2–500 nm range [19]. Dynamic light scattering is a method that relies on light interaction. The dynamic light scattering (DLS) analysis of the CSNP-SiO_2 nanocomposite shows a particle diameter average of 75 nm with a polydispersity index of 0.382.

Scanning Electron Microscopy

As shown (Figure 5) in the SEM images, the undefined and whitish SiO2 nanoparticles are dispersed uniformly within the silicone elastomer specimens. The nano-SiO_2 concentrations were distributed uniformly throughout the silicone specimens, according to SEM analysis. As the SiO_2 nanoparticles loading were increased in all specimens, no aggregates were detected.

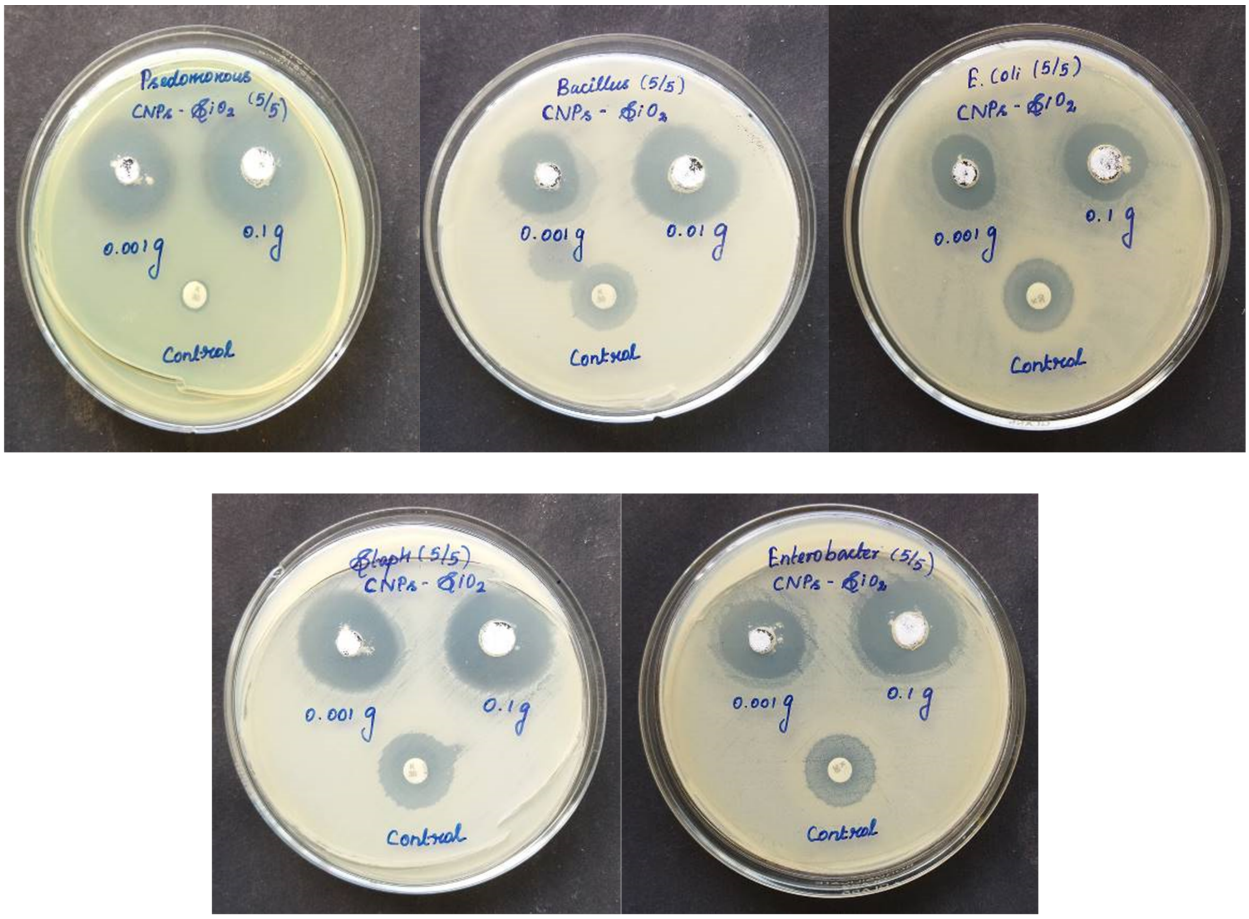

Figure 9: Zone of inhibition of CSNP-SiO_2 against various bacterial strains

The morphology of the CSNP-SiO_2 nanocomposite was determined using scanning electron microscopy. Because of the polymeric nature of CS and SiO_2 on the polymer matrix, the CSNP-SiO_2 has an undefined shape with agglomeration. At (20 and 2lm) magnification. The surface morphology and uniform distribution of CSNP-SiO_2 nanocomposite in the polymer nanocomposite are spherical, as shown in Figure 5, as is the shape of encapsulated nanoparticles in the polymer nanocomposite (Figure 5). SEM images can create a histogram with Image J software to determine the nanoparticle's small size and even distribution [20]. Scanning electron microscopy studies show that the cross-linked SiO_2 materials have a larger surface area and more variable morphology.

Absorbance spectra

UV-Visible spectroscopy is used to examine the optical properties of the CSNP-SiO_2 nanocomposite, which are plotted in Figure 6. A UV-visible spectrum of CSNP-SiO_2 nanocomposite revealed a broad absorption peak in the visible region at 380 nm. The adsorption behaviours at 380 nm indicate the presence of interenergetic bands between the conduction and valence bands of CSNPs, as well

Table 1: FTIR Peak value and corresponding function groups

S. No	Peak (cm^{-1})	Functional Group
1	3444	-NH_2 and -OH stretching primary amine
2	2921	C–H stretch alkanes
3	1631	C=C stretching alkene
4	1094	C-O stretching aliphatic ether
5	794	C=C bending alkene

Table 2: Zone of inhibition of CSNP-SiO_2 against selected bacterial strains

Bacterial Strains	Zone of Inhibition (mm in diameter) Concentration		
	0.01 g	0.1 g	Control
Bacillus sp	2.0	2.2	1.6
E.coli	1.6	2.0	1.8
Enterobactersp	2.1	2.6	1.8
Staphylococuus aureus	2.6	2.9	1.8
Pseudomonas sp	2.2	2.5	0.8

as the formation of CSNPs [21]. In other words, the wavelength difference of CSNP may be affected by its concentration [22]. As a nucleation and stabiliser controller, the polysaccharide may control these changes in particle size and morphology.

Effect of Fluorescence Spectra

Figure 7 depicts the fluorescence spectra of a CSNP-SiO_2 nanocomposite measured with an excitation wavelength. The Fluorescence (FL) band's centre appears at 608 nm. The fluorescence intensity increased as the size of the CSNP-SiO_2 nanocomposite increased. The intensity of the fluorescence emission band and the absorption band of the CSNP-SiO_2 nanocomposite were concentration and particle size dependent.

Thermogravimetric Analysis

The thermogravimetric analysis was used to assess the thermal stability of the composites. In a nitrogen atmosphere, the temperature of decomposition of the samples was investigated. TGA curves for chitosan and chitosan-SiO_2 are shown in Figure 8. Thermal decomposition parameters were calculated using the TGA curves. Figure 8 shows data for CSNP-SiO_2 nanocomposite from 50 to 650 °C at a heating rate of 10 °C/min. In general, all samples degrade in two stages: I water molecule loss and (ii) organic polymer material decomposition [23].

CSNP-SiO_2 loses weight in two stages at temperatures ranging from 50 to 630 °C. The first weight loss (4.8mg) for CSNP-SiO_2 occurred at 50–180 °C due to chitosan dehydration-induced evaporation of water molecules. Polymer chain decomposition is responsible for the second weight loss step (3.7 mg) at 200–420°C [24]. This shows that the chitosan/silica hybrid is completely involved in cross linking, and the results clearly show that it loses less weight than neat chitosan. The TGA plot clearly shows that chitosan and its composites degrade differently. The addition of the SiO_2 inorganic particle to the biopolymer chitosan improved the thermal stability of the composites, according to TGA results.

Antibacterial Activity

Chitosan stabilizer, a naturally occurring polymer, was added in various amounts to the prepared silicon dioxide nanoparticles to produce Chitosan- Silicon dioxide with varying silicon dioxide percentages for long-term stability, prevention of nanoparticle agglomeration, and enhancement of antibacterial efficacy. The CSNP-SiO_2 antibacterial activity was tested against five clinical pathogenic bacteria. Gram-positive *Bacillus subtilis*, *Staphylococcus aureus*, and Gram-negative *Escherichia coli, Psedomonous*, and *Enterobacter* strains were tested for antibacterial activity of the CSNP-SiO_2 nanocomposite.Figure 9 depicts a distinct Zone of Inhibition (ZOI) surrounding the CSNP-SiO_2 on culture-loaded MHA plates, indicating antibacterial efficacy. The mechanism underlying chitosan's antibacterial activity can be described as the interaction of positive charges in chitosan, such as protonated NH_3 with negative charges in bacteria's cell walls via electrostatic forces. These interactions disrupt the function of the microbial cell membrane, preventing intracellular compounds from escaping and preventing nutrient transformation, ultimately killing the bacteria [7, 25]. *Staphylococcus aureus and Enterobacter* had the highest susceptibility at 24 and 48 hours, with zones of inhibition of 2.9 mm and 2.6 mm respectively. Psedomonous and Bacillus subtilis had the highest susceptibility to CSNP-SiO_2 at 24 h, with zones of inhibition of 2.5 and 2.2 mm respectively, while Escherichia coli had the lowest zone of inhibition of 2.0 mm.

CONCLUSIONS

The properties of a novel chitosan-SiO_2 nanocomposite were investigated after its successful synthesis. The XRD results show that increasing the spacing of SiO_2 resulted in an intercalated structure. The FTIR spectra of all the composites show the presence of distinct organic and inorganic absorption bands. According to TGA results, the addition of chitosan-SiO_2 nanocomposite particles to biopolymer chitosan improved the thermal stability of the composites. The prepared samples were tested for antibacterial activity against gram-positive *Bacillus subtilis* and *Staphylococcus aureus* bacteria strains as well as gram-negative *Enterobacter, Escherichia coli*, and *Pseudomonas fluorescens* bacteria strains using the suitable diffusion method. The results of the characterization demonstrated the formation of a CSNP-SiO_2 nanocomposite. The antibacterial results confirmed that all the samples were antibacterial against the bacteria strains. Based on the findings, the CSNP-SiO_2 nanocomposites could be an effective antibacterial agent against dangerous bacterial pathogens.

ACKNOWLEDGEMENT

Rajaduraipandian Subramanian (Register No: 20111232031009) thanks to the research centre Sri Paramakalyani College, Manonmaniam Sundaranar University, Alwarkurichi - 627412 for their assistance with this research.

Funding Support

The authors declare that they have no funding sup-

port for this study.

Conflict of Interest

The authors declare that they have no conflict of interest.

REFERENCES

[1] M Rehan, M E El-Naggar, H M Mashaly, and R Wilken. Nanocomposites based on chitosan/silver/clay for durable multi-functional properties of cotton fabrics. *Carbohydrate Polymers*, 182:29–41, 2018.

[2] M H Kafshgari, A Mazare, M Distaso, W H Goldmann, W Peukert, B Fabry, and P Schmuki. Intracellular Drug Delivery with Anodic Titanium Dioxide Nanotubes and Nanocylinders. *ACS Applied Materials & Interfaces*, 11(16):14980–14985, 2019.

[3] Ahmad Bhat, S Zafar, F Ullah Mirza, A Hossain Mondal, A Kareem, A Mohd, Q Haq, and N Nishat. NiO nanoparticle doped-PVA-MF polymer nanocomposites: Preparation, Congo red dye adsorption and antibacterial activity. *Arabian Journal of Chemistry*, 13(6):5724–5739, 2020.

[4] P G Luo and F J Stutzenberger. Nanotechnology in the detection and control of microorganisms. *Advances in Applied Microbiology*, 63:145–181, 2008.

[5] A S Shabunin, V E Yudin, I P Dobrovolskaya, E V Zinovyev, V Zubov, E M Ivan'kova, and P Morganti. Composite Wound Dressing Based on Chitin/Chitosan Nanofibers: Processing and Biomedical Applications. *Cosmetics*, 6(1):16–16, 2019.

[6] L Cremar, J Gutierrez, J Martinez, L Materon, R Gilkerson, F Xu, and K Lozano. Development of antimicrobial chitosan based nanofiber dressings for wound healing applications. *Nanomedicine Journal*, 5(1):6–14, 2018.

[7] N Liu, X G Chen, H J Park, C G Liu, C S Liu, X H Meng, and L J Yu. Effect of MW and concentration of chitosan on antibacterial activity of Escherichia coli. *Carbohydrate Polymers*, 64(1):60–65, 2006.

[8] M D Alba, A Cota, F J Osuna, E Pavón, A C Perdigón, and F Raffin. Bio nanocomposites based on chitosan intercalation in designed swelling high-charged micas. *Scientific Reports*, 9(1):10265–10265, 2019.

[9] M S Alshammari, A A Essawy, A M El-Naggar, and S M Sayyah. Ultrasonic-Assisted Synthesis and Characterization of Chitosan-Graft-Substituted Polyanilines: Promise Bio-Based Nanoparticles for Dye Removal and Bacterial Disinfection. *Journal of Chemistry*, 2020.

[10] X Wang, X Liu, C Xiao, H Zhao, M Zhang, N Zheng, and J Lu. Triethylenetetramine-modified hollow Fe3O4/SiO2/chitosan magnetic nanocomposites to remove Cr (VI) ions with high adsorption capacity and rapid rate. *Microporous and Mesoporous Materials*, 297:110041–110041, 2020.

[11] S Preethi, K Abarna, M Nithyasri, P Kishore, K Deepika, R Ranjith Kumar, and D Bharathi. Synthesis and characterization of chitosan/zinc oxide nanocomposite for antibacterial activity onto cotton fabrics and dye degradation applications. *International Journal of Biological Macromolecules*, 164:2779–2787, 2020.

[12] M Chandrasekaran, K D Kim, and S C Chun. Antibacterial Activity of Chitosan Nanoparticles: A Review. *Processes*, 8:1173–1173, 2020.

[13] B Li, T Su, X Chen, B Liu, B Zhu, Y Fang, and G Xie. Effect of chitosan solution on the bacterial septicemia disease of Bombyx mori (Lepidoptera: Bombycidae) caused by Serratia marcescens. *Applied Entomology and Zoology*, 45(1):145–152, 2010.

[14] F Al-Sagheer and S Muslim. Thermal and mechanical properties of chitosan/SiO2 hybrid composites. *Journal of Nanomaterials*, 3:1–3, 2010.

[15] A M Meftah, E Gharibshahi, N Soltani, W M M Yunus, and E Saion. Structural, Optical and Electrical Properties of PVA/PANI/Nickel Nanocomposites Synthesized by Gamma Radiolytic Method. *Polymers*, 6(9):2435–2450, 2014.

[16] A Sorrentino, G Gorrasi, and V Vittoria. Potential perspectives of bio-nanocomposites for food packaging applications. *Food Science & Technology*, 18:84–95, 2007.

[17] C Paluszkiewicz, E Stodolak, M Hasik, and M Blazewicz. FT-IR study of montmorillonite-chitosan nanocomposite materials. *Spectrochimica Acta Part A: Molecular and Biomolecular Spectroscopy*, 79(4):784–788, 2011.

[18] B Akbari, M P Tavandashti, and M Zandrahimi. Particle size characterization of nanoparticles – a practical approach. *Iranian Journal of Materials Science and Engineering*, 8(2):48–56, 2011. ISSN: 1735-0808.

[19] A Longo, G Carotenuto, M Palomba, and

S D Nicola. Dependence of Optical and Microstructure Properties of Thiol-Capped Silver Nanoparticles Embedded in Polymeric Matrix. *Polymers*, 3(4):1794–1804, 2011.

[20] Hailan Xu, Haowei Shi, Yuxiang Yang, and Xiangnong Li. Synthesis and characterization of nanocomposites Fe3O4-SiO2-chitosan based on lbl technology. *Glass Physics and Chemistry*, 42(3):312–321, 2016.

[21] A El Mragui, O Zegaoui, and J C G Silva. Elucidation of the photocatalytic degradation mechanism of an azo dye under visible light in the presence of cobalt doped TiO2 nanomaterials. *Chemosphere*, 266:128931–128931, 2021.

[22] A Saravanakumar and M Dharmendirakumar. Synthesis and characterization of SiO2-Chitosan supported AgNPs and its catalytic application for reduction of malachite green. *Indian J. Chem. Technol*, 25(7):546–552, 2018.

[23] M Abbasi. Synthesis and characterization of magnetic nanocomposite of chitosan/SiO2/carbon nanotubes and its application for dyes removal. *Journal of Cleaner Production*, 145:105–113, 2017.

[24] M E Mahmoud, G M Nabil, H Abdel-Aal, N A Fekry, and M M Osman. Imprinting "Nano-SiO2-Crosslinked Chitosan-Nano-TiO2" Polymeric Nanocomposite for Selective and Instantaneous Microwave-Assisted Sorption of Hg(II) and Cu(II). *ACS Sustainable Chemistry & Engineering*, 6(4):4564–4573, 2018.

[25] S P Pasaribu, J Kaban, M Ginting, and K R Sinaga. Synthesis and evaluation antibacterial activity of phosphate buffer solution (pH 7.4) - soluble acylated chitosan derivative. *AIP Conference Proceedings*, 2049(1), 2018.